

# GraspLDM: Generative 6-DoF Grasp Synthesis using Latent Diffusion Models

Kuldeep R Barad<sup>1,2</sup>, Andrej Orsula<sup>1</sup>, Antoine Richard<sup>1</sup>, Jan Dentler<sup>2</sup>, Miguel Olivares-Mendez<sup>1</sup> and Carol Martinez<sup>1</sup>

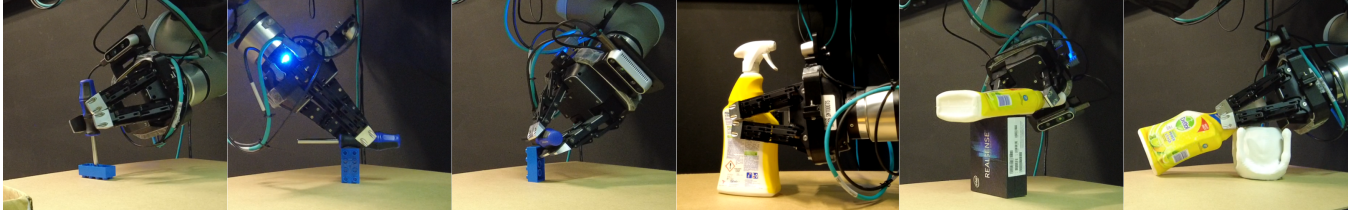


Fig. 0: GraspLDM models trained on synthetic data successfully transfer to the real world and provide stable 6-DoF grasps from single-view RGB-D data in the presence of workspace and motion planning constraints.

**Abstract**—Vision-based grasping of unknown objects in unstructured environments is a key challenge for autonomous robotic manipulation. A practical grasp synthesis system is required to generate a diverse set of 6-DoF grasps from which a task-relevant grasp can be executed. Although generative models are suitable for learning such complex data distributions, existing models have limitations in grasp quality, long training times, and a lack of flexibility for task-specific generation. In this work, we present GraspLDM—a modular generative framework for 6-DoF grasp synthesis that uses diffusion models as priors in the latent space of a VAE. GraspLDM learns a generative model of object-centric  $SE(3)$  grasp poses conditioned on point clouds. GraspLDM’s architecture enables us to train task-specific models efficiently by only re-training a small de-noising network in the low-dimensional latent space, as opposed to existing models that need expensive re-training. Our framework provides robust and scalable models on both full and single-view point clouds. GraspLDM models trained with simulation data transfer well to the real world and provide an 80% success rate for 80 grasp attempts of diverse test objects, improving over existing generative models. We make our implementation available at <https://github.com/kuldeepbrd1/graspldm>.

## I. INTRODUCTION

Robotic grasping of unknown objects from visual observations is an integral skill for autonomous manipulation systems in the real world. Grasping is the fundamental manipulation task of generating restraining contacts on an object. An essential part of this task is grasp synthesis, which involves reasoning about a set of grasps that are possible around an object. From this set of possible grasps, a subjectively good grasp can then be chosen based on grasp quality, task context, and kinematic feasibility. Vision-based grasp synthesis is a challenging problem for three main reasons. First, there are infinite possible grasps on any object and the distribution of good grasps can be complex, with multiple modes and discontinuities. Second,

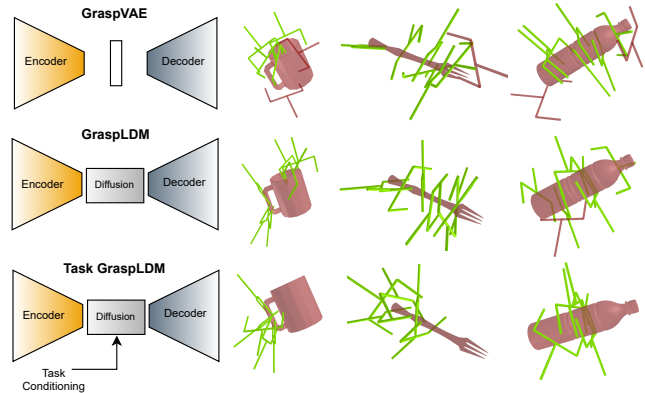


Fig. 1: GraspLDM uses a de-noising diffusion model in the latent space of a VAE to improve grasp generation performance. It also enables injection of task-conditional guidance in a modular manner.

the grasp generation process has to rely on unstructured visual observations from the sensors. Finally, it needs to generalize to an arbitrary set of unknown objects that a robot may encounter in the real world. To alleviate some of these issues, recent works [1] have proposed to use learning-based approaches. While generating 6-Degrees of Freedom (DoF) poses remains difficult [2], a simplification of this problem to tabletop objects, leading to a 4-DoF grasping space, has shown promising results.

In this work, we focus on generating object-centric 6-DoF grasps using point clouds. We assume a parallel jaw gripper and parameterize a grasp by its  $SE(3)$  pose. The objective is to learn a representation of object-centric 6-DoF grasps that can generalize to unknown objects. Learning this representation is difficult, as the model must reason about an arbitrary set of grasp poses for each object in the  $SE(3)$  space. Deep generative models are suitable for this problem, as they are designed to learn complex data-generating distributions efficiently. 6DoF-Graspnet [3], a primary generative grasp synthesis model, learns the distribution of object-

<sup>1</sup>Space Robotics Research Group (SpaceR), Interdisciplinary Centre for Security, Reliability and Trust (SnT), University of Luxembourg, Luxembourg. [kuldeep.barad@uni.lu](mailto:kuldeep.barad@uni.lu)

<sup>2</sup>Redwire Space Europe, Luxembourg

centric grasps in a continuous latent space of a conditional Variational Autoencoder (VAE). However, the VAE exhibits poor sampling quality, which can be attributed to the prior gap problem in VAEs when the encoding distribution does not match the prior very well [4]. On the other hand, diffusion models [5], [6] are a class of generative models that can overcome these problems. In particular, the latent diffusion [7] formulation provides an efficient and flexible generation architecture by using a diffusion model in the latent space of a VAE.

In this work, we propose GraspLDM - a learning-based generative modeling approach for 6-DoF grasp synthesis. GraspLDM learns the distribution of successful grasps on object point clouds using latent diffusion similar to [8], that transfers to the real world (Fig. 0). In GraspLDM, a diffusion model is trained efficiently inside the low-dimensional latent space of a VAE. This diffusion model acts as a prior and bridges the gap between the VAE prior and the posterior distribution fit during the training. Using diffusion in the latent space improves the quality of sampled grasps and avoids the representational complexity of operating directly on pairs of point clouds and grasp pose. It also enables two aspects of model flexibility that are not available in grasp synthesis models based on VAE [3] and diffusion [9]. First, task-specific conditional guidance can be provided solely in the latent space without re-training the VAE encoder and decoder. Second, multiple diffusion models can be trained efficiently and plugged inside this low-dimensional latent space.

In summary, our work makes three contributions. **(1) We introduce a new generative modeling framework for 6-DoF grasp synthesis using latent diffusion.** To the best of our knowledge, no other work has applied latent diffusion for 6-DoF grasp synthesis for scalable real-world parallel-jaw grasping. **(2) We show that a diffusion model in the latent space improves the grasp sample quality of a standard VAE model.** In simulation tests, our latent diffusion models improve generation performance. Further, they transfer to the real world to provide more stable grasps from single-view point clouds. **(3) We demonstrate that our architecture enables the injection of task-specific conditioning in generation with limited additional training effort.** The separation of VAE and diffusion model introduces flexibility that allows rapid training of task-specific models in the latent space.

## II. RELATED WORK

### A. 6-DoF Grasp Synthesis

Grasp synthesis was already studied by [10] using analytical methods, which rely on the knowledge of object models and properties that are rarely available in the real world. Today, grasp synthesis is framed as the problem of finding stable grasp poses from sensor data, subject to a gripper. Data-driven and learning-based methods have made notable progress, especially on 4-DoF planar grasp synthesis using parallel and vacuum grippers. In contrast, generalizable 6-DoF grasp synthesis is an active research topic [2] with

two broad classes: discriminative and generative approaches. Discriminative approaches rely on a manual pose sampling strategy and learn to discriminate good grasps from bad grasps using a quality measure [11]. Generative approaches instead directly learn to generate grasp poses from an observation [3], [12] with implicit sampling. Since grasps can be sampled directly from the learned model [3] these tend to be efficient. Some works on 6-DoF grasping also address auxiliary tasks to improve grasp generation, like shape completion and 3D reconstruction [13]. In this work, we present a generative approach that learns a continuous distribution of object-centric grasps conditioned on point clouds in an end-to-end manner.

### B. Generative Models for Grasp Synthesis

A conditional VAE [14] was introduced in [3] to learn a point cloud conditioned distribution of good grasps in a continuous latent space, from which they can be efficiently sampled. While the VAE is successfully able to cover multiple grasp modes, VAE alone provides a large fraction of unsuccessful grasps when executed. Consequently, additional stages for pose refinement are required. [15] builds upon [3] with an additional stage of collision checking using a learned network. However, VAEs underperform against discrete regression models [12]. GraspLDM improves the generative performance over VAE-based methods using latent diffusion.

### C. Denoising Diffusion Models

GraspLDM utilizes a diffusion model based on Denoising Diffusion Probabilistic Models (DDPM) [6]. Score-based Generative Model (SGM) [5] and Stochastic Differential Equations (SDE) are equivalent formulations of the diffusion process with notable implementation differences. For grasp pose generation, [9] uses the SGM formulation and learns a scalar field representing the denoising score. While their models effectively refine randomly sampled SE(3) grasp poses to low-cost (good grasp) regions, the analysis only presents learning on full point clouds of a single category (Mugs). Real-world tests on Mugs in [9] use ground truth pose of the object. Further, Langevin-type sampling is slow and the model needs to be retrained for downstream tasks. In contrast, GraspLDM is a more flexible formulation to [9] that operates a diffusion model on a vector field in the continuous latent space of a VAE. Our analyses and validation are also more extensive using full and partial point clouds from a large object category set, complemented with real-world transfer tests. GraspLDM can also use fast samplers like Denoising Diffusion Implicit Model (DDIM) as a drop-in replacement post-hoc with minimal performance loss. Further, GraspLDM can be extended to gripper parameterizations beyond the pose, in contrast to [9]. Diffusion models have also been utilized for dexterous grasp synthesis [16], but rely on the availability of the object model.

## III. GRASP LATENT DIFFUSION MODELS

We consider the problem of generating 6-DoF grasps on unknown object point clouds. We cast it as a generative modeling problem that is concerned with learning the conditional

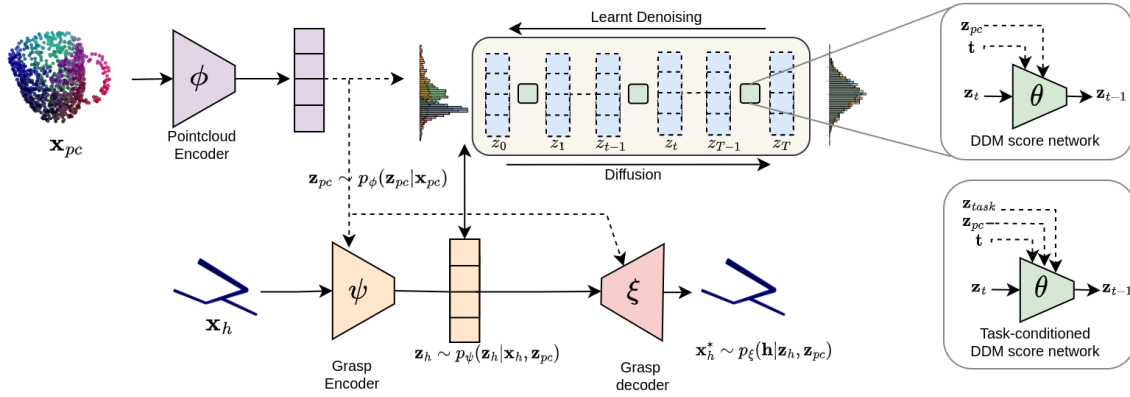


Fig. 2: Grasp Latent Diffusion Model (GraspLDM) is composed of a point cloud encoder ( $\phi$ ), a grasp encoder ( $\psi$ ), a grasp decoder ( $\xi$ ), and a latent diffusion module using a score network ( $\theta$ ). The point cloud encoder encodes a point cloud into a shape latent ( $\mathbf{z}_{pc}$ ). At test time, the grasp encoder is not required and we sample the grasp latent  $\mathbf{z}_h$  directly from the prior distribution. This latent goes through reverse diffusion before decoding. For task conditional generation, we modify the diffusion score network to accept task context  $\mathbf{z}_{task}$ .

distribution  $p(\mathbf{H}^* | \mathbf{x}_{pc})$ , where  $\mathbf{H}^*$  is a set of successful grasp poses  $H \in SE(3)$ , given a point cloud  $\mathbf{x}_{pc} \in \mathbb{R}^3$ . Learning effective generalizable representations to model this distribution is difficult because of its complexity in  $SE(3)$  space. To tackle this, we propose to learn a latent variable model  $p(H | \mathbf{z}, \mathbf{x}_{pc})$ , where  $\mathbf{z}$  represents the latent, by maximizing the likelihood of the training data consisting of successful grasps.

$$p(H | \mathbf{x}_{pc}) = \int p(H | \mathbf{z}, \mathbf{x}_{pc}) p(\mathbf{z}) d\mathbf{z} \quad (1)$$

Since we do not have access to the real latent space, computing the likelihood of data over the whole latent space in Eq. 1 is intractable. To overcome this, we use a VAE formulation for learning our generative model. VAE’s encoder compresses the complex point cloud-grasp pair input to a continuous latent space with a prior distribution. However, the approximate posterior of the encoder does not match the prior perfectly, especially if it prioritizes data reconstruction for grasp accuracy. To tackle this, we use a diffusion model in its latent space. Together, they form the latent diffusion model for grasp generation that we call GraspLDM. The diffusion model simultaneously improves sample quality by bridging the prior gap in the latent space and enables the introduction of latent space guidance with task context. The following sections describe the GraspLDM design in detail.

### A. Conditional Variational Autoencoder

Our conditional VAE structure consists of a point cloud encoder ( $\phi$ ), a grasp pose encoder ( $\psi$ ), and a grasp pose decoder ( $\xi$ ) as shown in Fig. 2. We use the point cloud encoder  $q_\phi(\mathbf{z}_{pc} | \mathbf{x}_{pc}) : \mathbf{x}_{pc} \in \mathbb{R}^{3 \times n} \mapsto \mathbb{R}^m$  that can operate on unordered point-sets of size  $n \in \mathbb{N}^+$  to provide a fixed size latent ( $\mathbf{z}_{pc}$ ) of size  $m \in \mathbb{N}^+$  called the shape latent. The shape latent is used as conditioning in the grasp pose encoder  $p_\psi(\mathbf{z}_h | H, \mathbf{z}_{pc})$  and the grasp pose decoder  $p_\xi(H | \mathbf{z}_h, \mathbf{z}_{pc})$ .  $\mathbf{z}_h$  is the conditional grasp latent at the VAE bottleneck. Finally, the model is trained by jointly optimizing the parameters

( $\psi, \theta, \xi$ ) of the encoders and decoders to maximize the Evidence Lower Bound (ELBO) [14]:

$$\mathcal{L}_{ELBO}(\phi, \psi, \xi) = \mathbb{E} \left[ \log p_\xi(H^* | \mathbf{z}_h, \mathbf{z}_{pc}) - \lambda D_{KL}(q_\psi(\mathbf{z}_h | H, \mathbf{z}_{pc}) || \mathcal{N}(\mathbf{0}, \mathbf{I})) \right] \quad (2)$$

In Eq. 2, the first term is the likelihood of the decoder reconstructing the input data. The second term measures the divergence between the approximate posterior distribution  $q_\psi(\mathbf{z}_h | H, \mathbf{x}_{pc})$  of the encoder and the assumed prior,  $\mathbf{z} \sim \mathcal{N}(\mathbf{0}, \mathbf{1})$ .  $\lambda$  is the weighting hyperparameter that controls the strength of KL regularization in the latent space. A constant  $\lambda = 1$  provides the strict ELBO objective. However, this frequently results in KL divergence term ( $D_{KL}$ ) becoming vanishingly small early in the training. When this happens, the conditional decoder becomes auto-regressive and the latent has no effect on the output [4]. To avoid this, we use linear annealing on the  $\lambda$  parameter.

### B. Latent Diffusion

In principle, sampling from VAE’s prior and decoding it should be sufficient to generate successful grasps. However, decoding a latent drawn from the prior often results in lower sample quality because of the prior gap problem highlighted earlier. To alleviate this issue, we propose to use a Denoising Diffusion Model (DDM) in the latent space. We justify the choice of latent diffusion structure from two observations. First, a simple DDPM would need to encode a point cloud at each step and use a high-dimensional intermediate representation, increasing computation for each denoising step. Alternatively, separating the point cloud encoder from the diffusion requires separate expensive training of a point cloud auto-encoder. Further, such a model needs to be re-trained for newer task conditionings.

A DDM consists of two processes: a forward diffusion process and a reverse de-noising process. In this work, we use the standard discrete-time DDPM [6], where the forward process is a linear Markov chain of deterministic

Gaussian kernels in Eq. 3a. The noise added at each time-step  $t \in [1, T]$  is pre-defined by a variance schedule  $\beta_t$ . We use linearly increasing  $\beta_t$  such that the distribution  $q(\mathbf{z}_T)$  converges to the standard normal distribution at the final forward time step  $T$ . In the forward diffusion process, a noisy sample at any time step can then be obtained by Eq. 3b.

$$q(\mathbf{z}_t|\mathbf{z}_{t-1}) = \mathcal{N}(\sqrt{1 - \beta_t}\mathbf{z}_{t-1}, \beta_t\mathbf{I}) \quad (3a)$$

$$\mathbf{z}_t = \sqrt{\bar{\alpha}_t}\mathbf{z}_0 + (1 - \bar{\alpha}_t)\boldsymbol{\epsilon}; \quad (3b)$$

$$\bar{\alpha}_t = \prod_{s=1}^t (1 - \beta_s) \quad ; \quad \boldsymbol{\epsilon} \sim \mathcal{N}(\mathbf{0}, \mathbf{I})$$

Intuitively, the forward diffusion process adds noise to input data until the data distribution transitions to a simple prior distribution. Consequently, recovering the data distribution from the prior requires a time reversal of the forward process from  $t = T$  to  $t = 0$ . This reverse diffusion process uses a learned score network ( $\theta$ ) which de-noises a sample, in our case the latent  $\mathbf{z}_h$ , from  $t$  to  $t - 1$ . For notational simplicity, we use  $\mathbf{z}_t$  to refer to conditional grasp latent  $\mathbf{z}_h$  at time  $t$ . Using the reverse diffusion kernel in Eq. 4, the distribution of the de-noised sample at time-step  $t - 1$  can be modeled by the mean  $\mu_\theta(z_t, t)$  and a known variance  $\sigma_t^2$ . More simply, we can re-parameterize the mean and instead learn a network to directly predict the noise  $\boldsymbol{\epsilon}_\theta(\mathbf{z}_t, t)$  to be removed at each step [6]. The de-noising score model  $\boldsymbol{\epsilon}_\theta$  predicts the noise to be removed conditioned on the current time-step, while the parameter weights ( $\theta$ ) are shared across all the time steps. Then, the sampling can be done using Eq. 5, where  $\sigma_t$  can be simplified to use variance similar to the forward process i.e.  $\beta_t$ . DDMs with this formulation can be trained to maximize an ELBO-like objective. Given the simplified formulation in [6] and adapting it to our latent diffusion architecture, this objective  $\mathcal{L}_D(\theta)$  can be written as Eq. 6.

$$p_\theta(\mathbf{z}_{t-1}|\mathbf{z}_t) = \mathcal{N}(\mu_\theta(z_t, t), \sigma_t^2\mathbf{I}) \quad (4)$$

$$\mathbf{z}_{t-1} = \frac{1}{\sqrt{1 - \beta_t}} \left( \mathbf{z}_t - \frac{\beta_t}{1 - \bar{\alpha}_t} \boldsymbol{\epsilon}_\theta(\mathbf{z}_t, t) + \sigma_t \boldsymbol{\eta} \right) \quad (5)$$

$$\mathcal{L}_D(\theta) = \mathbb{E} \|\boldsymbol{\epsilon}_t - \boldsymbol{\epsilon}_\theta(\mathbf{z}_{h,t}, \mathbf{z}_{h,0}, t)\|^2 \quad (6)$$

### C. Implementation Details

The training is done in two stages. In the first stage, we fit the parameters of encoders and decoders by maximizing the VAE ELBO in Eq. 2. In the second stage, we fit the parameters of the score model to minimize DDM loss in Eq. 6. While it is possible to train all the networks in a single stage, it is easier and faster to train the diffusion model once the latent space of the VAE is frozen. In single-stage training, the constantly changing posterior distribution at the encoder means that the optimization of the weights of the de-noising score network is wasteful until VAE training has converged sufficiently. To train our networks, we use objects and grasp annotations from the ACRONYM [17] dataset. We use train-test splits defined in [12]. We empirically choose the ELBO

modifying hyperparameter  $\lambda$ , which is annealed linearly from  $1e - 7$  to 0.1 for 50% of the training steps and then held constant until the end of training. This ensures that the KL term does not vanish in the early stages of the training while also enforcing lower regularization to prioritize grasp pose reconstruction during the later stages.

The point cloud encoder is based on Point-Voxel CNN (PVCNN) architecture [18] which is more efficient than conventionally used PointNet architecture [18]. The input to the point cloud encoder is fixed at 1024 points, to balance memory usage with point sampling density. The output of the point cloud encoder is a latent ( $\mathbf{z}_{pc}$ ) of size 128. The grasp pose encoder and decoder are 1D convolutional neural networks with residual blocks. Conditioning is done using FiLM [19], which uniquely scales and shifts the feature maps at every residual block based on the conditioning features. The decoder network is the same as the encoder but reversed, whose output is the reconstruction ( $\mathbf{x}_h^*$ ) of the input. The noise prediction network for diffusion is a residual network similar to the grasp encoder and is conditioned on both the diffusion time step ( $t$ ) and the shape latent ( $\mathbf{z}_{pc}$ ).

$$\mathbf{h} = [\mathbf{t}, \mathbf{a}]^T; \quad \mathbf{a} = \frac{4}{1 + q_w} [q_x, q_y, q_z]^T \quad (7)$$

We use the representation of the grasp pose ( $\mathbf{h}$ ) given in Eq. 7, where  $\mathbf{t}$  is the translation vector while  $\mathbf{a}$  is the Modified Rodrigues Parameters (MRP) [20] for orientation. Eq. 7 also relates MRP with quaternions where  $q_w$  is the quaternion scalar component. In contrast to regressing pose matrices or quaternion vectors that have one or more dependent parameters, the three parameters of MRPs can be regressed independently. We encourage readers to check the details of the implementation in our code release.

## IV. RESULTS AND DISCUSSION

### Evaluation

We evaluate the performance and scaling of our Gras-pLDM on two category sets- 1C and 63C, where C denotes the number of ShapeNetSem categories from the ACRONYM dataset. 1C is composed of 110 Mugs in the train set and 50 held-out Mugs in the test set. The 63C set contains 1100 objects from 63 categories in the train set and 400 held-out objects in the test set. For observations, we use full object point clouds and partial point clouds. Full object point clouds are sampled from the mesh surface. On the other hand, partial point clouds are rendered from a virtual depth camera at a distance between 30cm and 1m. In both cases, point clouds are randomly rotated, noised, and regularized to 1024 points which is the input to our point cloud encoder.

We evaluate *success rate* of the grasp poses generated by the models in a large-scale parallel simulation in Isaac Gym [21]. In the simulation, we use only a Franka-Emika two fingered gripper without the robotic arm and ignore gravity to avoid the effect of external factors on the evaluations. For each grasp pose, the simulation executes three steps to report a grasp success or a failure. (1) The gripper is spawned at the given grasp pose relative to the object with the fingers



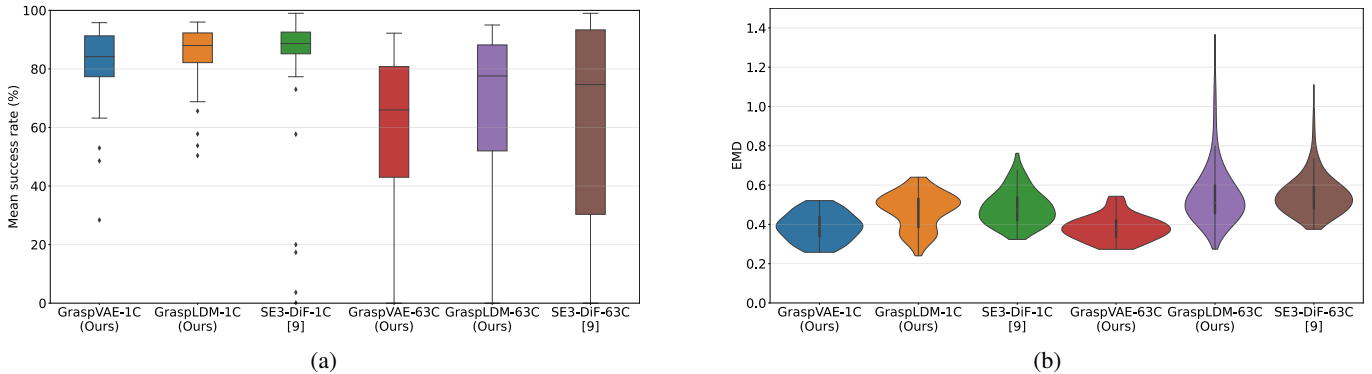


Fig. 3: Grasp generation performance and scaling on full object point clouds ( $N = 1024$ ). (a) The mean *success rate* in simulation of 300 generated grasps poses per object. (b) SE(3) EMD between ground-truth grasp pose distribution and 100 sampled grasp poses (lower is better). SE3-DiF-1C and SE3-DiF-63C are the SE(3) Grasp Diffusion models from [9].

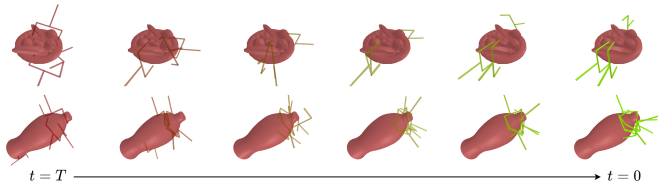


Fig. 4: Visualization of latent space de-noising in GraspLDM. Reverse diffusion de-noises these latents from  $t = T$  to  $t = 0$ , gradually moving the bad grasps towards regions of good grasps.

open. (2) The fingers are closed at the grasp pose. (3) The gripper lifts the object 1m in the +Z direction. Finally, a grasp is reported successful if the object remains attached to the gripper. Note that the evaluation is conservative as any penetration of the gripper in the first step or adverse contact in the second stage will result in a grasp failure. On the other hand, we observe that for many large objects, ground truth grasp poses in the ACRONYM dataset provide a very low or zero success rate. Therefore, we filter out the objects in each set for which the ground truth grasps fail more than 75% of the time.

While the success rate evaluates the quality of grasp generation, a model with a high success rate may generate grasps only around a small region of the object, instead of covering all the graspable regions around the object. Consequently, we also use SE(3) *Earth Mover’s Distance (EMD)* metric [9] to evaluate how well the trained models learn the object-centric grasp pose distribution. The SE(3) EMD metric evaluates the empirical distance between two distributions of SE(3) poses. To compute this, we sample 100 grasps per object from a model and sample 100 random grasps from the ground truth datasets. To further validate the flexibility of GraspLDM, we provide additional results on sampling speed and task-conditional generation.

#### A. 6-DoF grasp generation

Here, we evaluate the ability of GraspLDM models to learn the complex distribution of successful grasp poses on full object point clouds. For each object, we take 3 randomly

sampled and augmented point clouds and generate 100 grasps on each. We aggregate the simulation results from all 300 grasp attempts into a *mean grasp success rate* per object reported in Fig. 3a. To assess the benefits of adding the diffusion model, the success rate results of GraspLDM models are compared with the corresponding GraspVAE models, which is the base VAE model with the same weights. For the baseline, we use the SE(3) grasp diffusion model [9] (SE3-DiF-63C). To understand the scaling behavior, we present results from each network on 1C and 63C sets. Further, Fig. 3b reports the EMD metric that evaluates the ability to cover the distribution of grasps in the data.

For success rate, we outline two observations in Fig. 3a. First, the LDM models consistently improve upon the base VAE models, demonstrating that the sample quality improves by using a diffusion model in VAE’s latent space. Second, the success rate performance of GraspLDM models scales better to a larger object set (63C). Comparing the median of the success rate on the test set in Fig. 3a, GraspLDM-1C improves the median success rate to 88% compared to 84% of GraspVAE-1C. On the larger 63C set, the GraspLDM-63C model improves the median success rate to 78% compared to 66% from GraspVAE-63C. GraspLDM models also improve the interquartile range in each case. For the comparison against the baseline, SE3-DiF-1C model reports a median success rate of 89% which is comparable to 88% the GraspLDM-1C model. On the larger 63C set, we observe that the GraspLDM-63C model registers 78% median success rate and distinctly higher interquartile range compared to SE3-DiF-63C. Therefore, GraspLDM models scale more favorably to larger object sets compared to the state-of-the-art approaches. During the tests, we also observed that the models available from [9] do not hold out a test split and is trained on all objects. Therefore, the comparison to SE3-DiF models [9] is conservative, which emphasizes the performance of GraspLDM on withheld objects.

Overall, the results validate our hypothesis that a diffusion model in the latent space can bridge the prior gap in the latent space to provide higher-quality grasp pose samples. Fig. 4 visualizes this effect where the latent de-noising

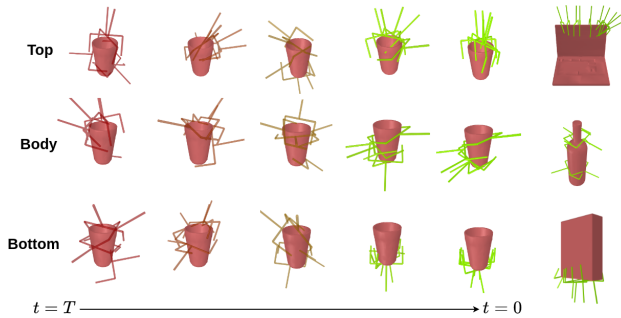


Fig. 5: Task-conditional de-noising in the latent space for a region-semantic class label (top, body, or bottom)

moves latents corresponding to bad grasps towards good grasp regions during the reverse diffusion process. In terms of grasp failures, we observe a major portion of them in large objects whose graspable regions are far from the center of mass. When lifted in simulation, the reaction torque snaps the object out of the gripper fingers and therefore is reported as a failure.

Fig. 3b shows that our models also register low EMD for most test objects, demonstrating good coverage of grasp modes in the ground truth data. The EMD performance of GraspVAE and GraspLDM models are comparable or marginally better than the state-of-the-art grasp diffusion models from [9]. However, the results show that while GraspLDM models effectively learn the grasp distribution, they have a slightly worse EMD compared to the GraspVAE models. We attribute this to two factors. First, reverse diffusion moves poor grasp poses (e.g. colliding or free-space grasps) towards a smaller number of high-density regions that tend to provide a higher success rate. Second, we follow the computation of SE(3) EMD from [9] by using cosine distance for rotation and metric Euclidean distance for translation. As a result, the EMD metric is more sensitive to the similarity in rotation despite translation having a potentially larger effect on the success of grasp execution.

### B. Conditional generation

For many manipulation tasks, the desired grasps are subject to a task context. Here, we demonstrate the flexibility of our architecture to provide this task context as conditional guidance in the latent space representing unconditional grasps. We do this by training a task-conditional diffusion model post hoc. For the proof-of-concept, we consider simple region-semantic labels "top", "body" and "bottom" as our conditioning signals. We use full point clouds of objects as inputs and pre-train a VAE without any task labels. We then include task labels only during the training of the diffusion model in the second stage. We associate a ground-truth class label of "top", "body" or "bottom" to each grasp based on whether the origin of the gripper's root is above, along, or below the unrotated object point cloud. We supply these labels to the diffusion model as an additional conditioning signal. We use a reduced subset of test objects for which these labels are meaningful (e.g. bottles) and remove those

TABLE I: Reverse diffusion sampling speed-up and performance of GraspLDM-63C. Standard DDPM (1000 steps) is compared with a fast sampler- DDIM (100 steps) for the number of grasps generated ( $N_G$ ) without re-training.

Sampling	$N_G = 100$ (s)	$N_G = 1000$ (s)	Median success rate
DDPM	$7.39 \pm 0.06$	$11.80 \pm 0.29$	<b>0.792</b>
DDIM	<b><math>0.75 \pm 0.02</math></b>	<b><math>1.14 \pm 0.01</math></b>	0.756
VAE	<b><math>0.02 \pm 0.01</math></b>	<b><math>0.03 \pm 0.01</math></b>	0.660

for which these labels are not relevant (e.g. plates). The final test set contains 200 unseen objects. We take pre-trained encoders and decoders from the GraspVAE-63C model and train the task-conditioned models (Task-GraspLDM) post-hoc, in less than 2 hours on a single NVIDIA V100 GPU.

At test time, we generate 50 grasps for each mode (top, bottom, and body) of an object. The input object point cloud is augmented with random rotations. To check whether the generated grasp complies with the input label, we reverse the rotation transformation and check the location of the gripper's root, as earlier. We report the precision between the labels of generated grasps and the labels supplied as conditioning. In this setting, the Task-GraspLDM model provides a mean precision of 0.703 averaged over all objects. We observe that the reverse diffusion process seamlessly moves a latent from a prior distribution to the desired task-conditional distribution, as visualized in Fig. 5. The tests show that GraspLDM allows effective injection of task conditioning post-hoc. Currently, the models are limited by the cases where there are no ground-truth grasps for a given label. For instance, if there are no 'bottom' grasp annotations for a laptop, the model generates grasps unconditionally all over the object. This can be addressed in future work along with more complex task contexts.

### C. Reverse diffusion sampling

A notable disadvantage of using DDPM-based grasp generation is the time to execute large number reverse sampling steps in a sequential manner. In DDPM, a large  $T$  is required to ensure that the Gaussian conditional distributions in Eq. 4 are a good approximation [22]. A Denoising Diffusion Implicit Model [23] assumes a non-Markovian forward process to speed up the sample generation and requires a lower number of sampling steps. Further, it can be used as a drop-in sampler to use with a score network trained on the DDPM objective in Eq. 6, without any re-training. To assess the performance and sampling speed trade-off, we take the GraspLDM-63C model and compare DDIM sampler with 100 steps with the naive DDPM sampler. Table I compares the execution time of the reverse diffusion loop in DDIM with the baseline 1000-step DDPM. Using DDIM sampling as a drop-in replacement, the sampling time drops to 0.75s for 100 grasps and 1.1s for 1000 grasps. This is 10x faster than DDPM with a small loss in success rate (3.6%). The experiment was conducted on a system with NVIDIA RTX 3080Ti GPU and Intel i7-12800H CPU. Given the rapid progress in creating fast reverse diffusion samplers, our pipeline provides the flexibility to trade-off speed against

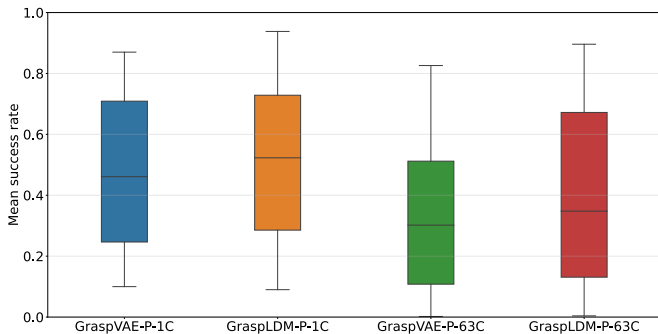


Fig. 6: Grasp generation performance on partial point clouds of 1C and 63C object sets.

performance for such diffusion samplers. In contrast, SE3-Grasp-DiF [9] models cannot leverage new samplers without re-training.

#### D. Single-view point clouds

For many real-world use cases, only single-view point clouds are available for grasp generation. Therefore, we also evaluate the GraspLDM framework’s ability to learn the distribution of grasps on noisy partial point clouds. For evaluation, we use the simulation environment as before, with the addition of a depth camera. The cameras are spawned randomly between 30cm and 1m from the object. We use the partial point cloud thus obtained to sample 25 grasps and execute them without filtering. For each object, we repeat these for 20 random camera poses. The success rate is reported in Fig. 6 for GraspVAE-P-1C, GraspLDM-P-1C, GraspVAE-P-63C, and GraspLDM-P-63C models, where ‘P’ implies that the model was trained on partial point clouds. In both cases, GraspLDM models improve the performance of the base VAE model. We found that for GraspLDM-P-63C models, higher capacity is required to compress a meaningful latent representation for 63C partial point clouds. We increase the grasp latent ( $z_h$ ) size to 16.

Note that we do not use preferential camera viewpoints, grasp filtering, or a support surface in the background. As a result, this evaluation provides a conservative metric for 6-DoF grasp-generation performance. This can be considered as the approximate lower bound of the grasp generation performance for real-world use cases. A large number of failures result from grasps that collide with parts of the objects not visible in the partial point clouds. Depending on the viewpoint, this occlusion confuses the model to see incomplete surfaces as edges along which the object could be grasped. For larger objects where grasps are concentrated in a small region of the object, these regions may not be available in a partial point cloud.

These issues highlight the need for discriminating bad grasps from good grasps for real-world tests. This can be done using a classification network on top of GraspLDM (as in real world tests in section IV-E) or preferably by adding a classification layer in the decoder. The latter problem of classifying grasps within the decoder of the current architecture, such that it can also be used for task-specific diffusion models, is out of the scope of the current work.

TABLE II: Real-world 6-DoF grasping success rate comparison on 16 evaluation objects in 5 random poses

Method	Success Rate
GraspLDM + GraspClassifier ( <i>ours</i> )	80%
GraspVAE + GraspClassifier ( <i>ours</i> )	76.25%
6-DoF Graspnet + Classifier [3]	37.5%

#### E. Real robot tests

To complement the large-scale evaluations conducted in simulation, we conduct thorough real-world tests to evaluate the performance of object-centric GraspLDM models. We assess the transfer on a hardware setup that consists of a 6-DoF UR-10e arm, a Robotiq-3F gripper, and an Intel Realsense D435 RGB-D camera. The gripper is used in a two-finger mode with the gripper sweep length restricted to 85mm to emulate the gripper used for generating the training data. The camera is mounted at the tool flange of the arm in an eye-in-hand configuration. We use a test set of 16 objects of diverse physical and geometric properties as shown in Fig. 7. Each grasping trial is conducted by placing a single object in a random pose on a table. We conducted five random pose trials per object to evaluate the success rate across a total of 80 grasp attempts without retries. The robot is set to an arbitrary fixed pose such that the camera boresight is approximately  $30^\circ$  to the table plane and directed approximately to the center of the table.

We use the GraspLDM-P-63C model introduced in section IV-D without any further fine-tuning. Since the model provides object-centric grasps, we use the segment-anything model [24] to segment the object in an RGB image. Subsequently, we mask the aligned depth image to provide a segmented object point cloud. This point cloud is provided to the model which generates 100 grasp candidates. Unlike simulation, real experiments require a grasp pose to be selected. For this purpose, we train a naive classifier (GraspClassifier) to provide a pseudo-probability of success for a given pair of a point cloud and a grasp pose. Subsequently, we rank and sort the grasps above a probability threshold ( $p > 0.5$ ). We attempt the grasps in the same order while checking for collision and kinematic failures. The first grasp with a valid plan is executed on the robot. During a grasp attempt, the robot first goes to a pre-grasp pose, which is offset from the grasp pose along the z-axis of the gripper. Then the gripper approaches the object along this axis and closes the fingers. Subsequently, the object is lifted and moved to a set pose above a bucket. A grasp is successful if all these steps are executed successfully. Together these steps test the validity of the grasp pose as well as the stability of the grasp in all axes.

For motion planning, we utilize an off-the-shelf RRTConnect planner. We use 6-DoF-Graspnet [3] as the real-world test baseline as it is a widely used grasp generation model. For a fair evaluation of grasp synthesis models, we only use the generator and classifier from [3] and do not include the iterative refinement stage, while keeping all other parts of the pipeline including segmentation the same as before. We compare this with GraspLDM-P-63C and GraspVAE-P-63C



in Table II. Grasp diffusion [9] is only trained on full point cloud models and therefore not used for comparison here.

Table II demonstrates that GraspLDM provides a superior grasp success rate in the real world while being entirely trained with simulation data. GraspLDM-P-63C model provides around 4.75% higher success rate over its base VAE model- GraspVAE-P-63C which also uses the same classifier. On the other hand, both our models provide a significantly higher success rate than 6-Dof-Graspnet [3] without its iterative refinement stage. We notice that high amounts of failure of the baseline result from grasps that collide with the object as well as from a lack of grasp generation diversity. In the latter case, it suffers from not producing enough grasps in kinematically feasible regions of the object in certain relative poses. We also observe a higher rate of planning failures for the baseline until a successful grasp is attempted, which is connected to grasp diversity. The results validate our architecture and training pipeline for practical applications. It is important to highlight that our models are only trained on 63 categories of a total of 180 in the ACRONYM dataset because of compute constraints. Therefore, we believe that the performance can be improved further.

## V. CONCLUSIONS

Learning generalizable representations for grasp generation is fundamental to robotic grasping. In this work, we propose GraspLDM- a novel generative framework for object-centric 6-DoF grasp synthesis using latent diffusion. Our architecture allows de-noising diffusion models to be used as expressive priors in the latent space of VAEs. This enables efficient learning of the complex distribution of object-centric 6-DoF grasp poses on point clouds. We conduct large-scale simulation tests to show that GraspLDM outperforms baseline methods and provides a 78% median success rate on our test set of 400 objects from 63 categories. GraspLDM shows good grasp generation performance while scaling favorably to large object sets compared to existing methods using generative modeling. Further, we validate our pipeline by training GraspLDM models on single-view point clouds generated in simulation and testing them in a real-world setup. GraspLDM demonstrates favorable transfer to the real world and provides 80% success rate on 16 test objects from single-view depth images. We further demonstrate the flexibility of our architecture to train efficient task-specific models and to use fast reverse diffusion samplers for downstream applications. GraspLDM can be extended to work with complex task conditionings and cluttered scenes.

## ACKNOWLEDGMENTS

This work is supported by the Fonds National de la Recherche (FNR) Industrial Fellowship grant (15799985) and Redwire Space Europe.

## REFERENCES

[1] J. Bohg *et al.*, “Data-driven grasp synthesis—a survey,” *IEEE Transactions on robotics*, 2013.  
 [2] R. Newbury *et al.*, “Deep learning approaches to grasp synthesis: A review,” *arXiv preprint arXiv:2207.02556*, 2022.



Fig. 7: Test object set containing objects with diverse visual, geometric and surface properties for real-world evaluation (left) and example grasps executed by GraspLDM (right)

[3] A. Mousavian *et al.*, “6-dof graspnet: Variational grasp generation for object manipulation,” in *Proceedings of the IEEE/CVF International Conference on Computer Vision*, 2019.  
 [4] S. Zhao *et al.*, “Infovae: Information maximizing variational autoencoders,” *arXiv preprint arXiv:1706.02262*, 2017.  
 [5] Y. Song *et al.*, “Generative modeling by estimating gradients of the data distribution,” *Advances in neural information processing systems*, 2019.  
 [6] J. Ho *et al.*, “Denosing diffusion probabilistic models,” *Advances in Neural Information Processing Systems*, 2020.  
 [7] R. Rombach *et al.*, “High-resolution image synthesis with latent diffusion models,” in *Proceedings of the IEEE/CVF Conference on Computer Vision and Pattern Recognition*, 2022.  
 [8] X. Zeng *et al.*, “Lion: Latent point diffusion models for 3d shape generation,” *arXiv preprint arXiv:2210.06978*, 2022.  
 [9] J. Urain *et al.*, “Se (3)-diffusionfields: Learning cost functions for joint grasp and motion optimization through diffusion,” *arXiv preprint arXiv:2209.03855*, 2022.  
 [10] A. Bicchi *et al.*, “Robotic grasping and contact: A review,” in *Proceedings 2000 ICRA. Millennium conference. IEEE international conference on robotics and automation. Symposia proceedings (Cat. No. 00CH37065)*. IEEE, 2000.  
 [11] J. Mahler *et al.*, “Dex-net 2.0: Deep learning to plan robust grasps with synthetic point clouds and analytic grasp metrics,” *arXiv preprint arXiv:1703.09312*, 2017.  
 [12] M. Sundermeyer *et al.*, “Contact-graspnet: Efficient 6-dof grasp generation in cluttered scenes,” in *2021 IEEE International Conference on Robotics and Automation (ICRA)*. IEEE, 2021.  
 [13] Z. Jiang *et al.*, “Synergies between affordance and geometry: 6-dof grasp detection via implicit representations,” *arXiv preprint arXiv:2104.01542*, 2021.  
 [14] D. P. Kingma *et al.*, “Auto-encoding variational bayes,” *arXiv preprint arXiv:1312.6114*, 2013.  
 [15] A. Murali *et al.*, “6-dof grasping for target-driven object manipulation in clutter,” in *2020 IEEE International Conference on Robotics and Automation (ICRA)*. IEEE, 2020.  
 [16] P. Li *et al.*, “Gendexgrasp: Generalizable dexterous grasping,” *arXiv preprint arXiv:2210.00722*, 2022.  
 [17] C. Eppner *et al.*, “Acronym: A large-scale grasp dataset based on simulation,” in *2021 IEEE International Conference on Robotics and Automation (ICRA)*. IEEE, 2021.  
 [18] Z. Liu *et al.*, “Point-voxel cnn for efficient 3d deep learning,” *Advances in Neural Information Processing Systems*, 2019.  
 [19] E. Perez *et al.*, “Film: Visual reasoning with a general conditioning layer,” in *Proceedings of the AAAI Conference on Artificial Intelligence*, 2018.  
 [20] J. L. Crassidis *et al.*, “Attitude estimation using modified rodrigues parameters,” in *Flight Mechanics/Estimation Theory Symposium 1996*, 1996.  
 [21] V. Makoviychuk *et al.*, “Isaac gym: High performance gpu-based physics simulation for robot learning,” *arXiv preprint arXiv:2108.10470*, 2021.  
 [22] J. Sohl-Dickstein *et al.*, “Deep unsupervised learning using nonequilibrium thermodynamics,” in *International Conference on Machine Learning*. PMLR, 2015.  
 [23] J. Song *et al.*, “Denosing diffusion implicit models,” *arXiv preprint arXiv:2010.02502*, 2020.  
 [24] A. Kirillov *et al.*, “Segment anything,” *arXiv preprint arXiv:2304.02643*, 2023.